An Upper Bound Limit Analysis to Determine the Stability of Slope Considering the Effect of Earthquake

Hai N. Le and An N. Chau
Ho Chi Minh City University of Technology, Ho Chi Minh, Vietnam
Email: nguyenhaile111@gmail.com, cnan@hcmut.edu.vn

***Abstract*—The cell-based smoothed finite element method (CS-FEM) and second order cone programming (SOCP) are used to access the seismic stability of slope in cohesive-frictional soil. In this study, the seismic force will be considered as the inertial load which calculated through horizontal acceleration factor α_h. The stability factor is expressed in the form of a dimensionless number $\gamma_{max}H\tan\phi/c$; where H is the slope height, γ_{max} and c are the maximum unit weight and cohesion of soil, respectively. In addition, the failure mechanisms of slope will be obtained directly from solving the optimization problems. A series of simulations are carried out and the results confirm that this numerical procedure provides stable and accurate solutions to seismic stabilities in compare with those using finite element method as well as the influence of the properties of soil to the slope stability.**

***Index Terms*—seismic, slope stability, CS-FEM, SOCP, limit analysis, upper bound**

I. Introduction

There are many approaches to solving geotechnical stability problems, including the seismic stability of slopes. One of the most powerful tool is to use limit theory, which estimates the ultimate load as well as failure mechanism. In this theory, upper bound or lower bound solution are used to determine the exact collapse load. However, the upper bound solution is usually employed, especially in geomechanic, because the kinematically admissible velocity field in upper bound analysis is easy to establish rigorously in comparison with the statically admissible stress field for lower bound solution.

Many researches have been applied the numerical method solution for the slope problems. Ref. [1] used the numerical method based on the upper bound theorem of perfect plastic solids to determine the stability of slope in static conditions and compared them with those of the experimental method. In the same conditions, [2] applied the finite element method based on the upper and lower bound theorem. However, little researches deal with the determination of the seismic stability of slope. In 2003, [3] used the numerical limit analysis method by applying to the problem of two-dimensional pseudo-static slope stability analysis based on upper and lower bound formulation.

This paper employ the cell-based smoothed finite element method (CS-FEM) with second-order cone programming (SOCP) to estimate the stability of slope in seismic conditions ([4-10]). A variety of examples will be carried out to evaluate soil properties as well as compared with the results of [3].

II. Problem Definition

A slope with height H tilted at a β angle in cohesive soil is illustrated in Fig. 1. The ground deformation takes place under plane strain. The slope is intended to determine the stability in the presence of horizontal seismic acceleration α_h. The stability of slope can be determined by a dimensionless factor $\gamma_{max}H\tan\phi/c$; where H is the slope height, γ_{max}, ϕ and c are the maximum unit weight, friction angle and cohesion of soil, respectively. The soil mass is assumed to be perfectly plastic, follow the Mohr-Coulomb failure criterion and an associated flow rule. Drained loading condition is also considered. Therefore, the values of cohesion (c) and friction angles (ϕ) should be corresponding to drained conditions, that is, c = c' and $\phi = \phi'$.

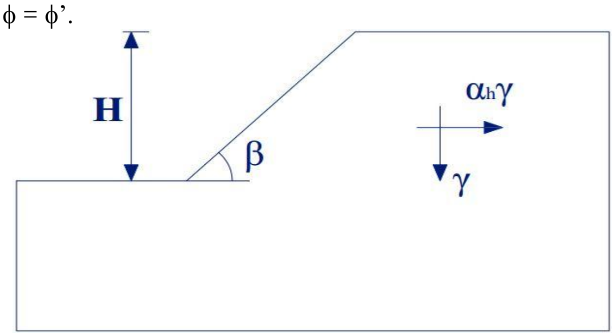

Figure 1. Definition of the problem

III. Upper Bound Limit Analysis Formulation

Consider a rigid-perfectly plastic body of area $\Omega \in R^2$ with boundary Γ, which is subjected to body forces $\boldsymbol{f}$ and to surfaces tractions $\boldsymbol{g}$ on the free portion Γ_t of Γ. The constrained boundary Γ_u is fixed and $\Gamma_u \cup \Gamma_t = \Gamma$,

Manuscript received July 3, 2017; revised November 1, 2017.

doi: 10.18178/ijscer.6.4.274-279

$\Gamma_u \cap \Gamma_t = \varnothing$. Let $\dot{\boldsymbol{u}} = [\dot{u} \quad \dot{v}]^T$ be plastic velocity or flow fields that belong to a space U of kinematically admissible velocity fields. Where $\dot{u}$ and $\dot{v}$ are the velocity components in the x and y directions respectively. The strain rates $\dot{\boldsymbol{\varepsilon}}$ can be expressed by relations

$$\dot{\boldsymbol{\varepsilon}} = \begin{bmatrix} \dot{\varepsilon}_{xx} \\ \dot{\varepsilon}_{yy} \\ \dot{\gamma}_{xy} \end{bmatrix} = \nabla \dot{\boldsymbol{u}} \tag{1}$$

with ∇ is the differential operator

$$\nabla = \begin{bmatrix} \dfrac{\partial}{\partial x} & 0 \\ 0 & \dfrac{\partial}{\partial y} \\ \dfrac{\partial}{\partial y} & \dfrac{\partial}{\partial x} \end{bmatrix} \tag{2}$$

The external work rate associated with a virtual plastic flow $\dot{\boldsymbol{u}}$ is expressed in the form as

$$W_{ext}(\dot{\boldsymbol{u}}) = \int_\Omega \boldsymbol{f}^T \dot{\boldsymbol{u}} d\Omega + \int_{\Gamma_t} \boldsymbol{g}^T \dot{\boldsymbol{u}} d\Gamma \tag{3}$$

The internal plastic dissipation of the two-dimensional domain Ω can be written as

$$W_{int}(\dot{\boldsymbol{\varepsilon}}) = \int_\Omega D(\dot{\boldsymbol{\varepsilon}}) d\Omega \tag{4}$$

where the plastic dissipation $D(\dot{\boldsymbol{\varepsilon}})$ is defined by

$$D(\dot{\boldsymbol{\varepsilon}}) = \max_{\psi(\sigma) \le 0} \boldsymbol{\sigma}.\dot{\boldsymbol{\varepsilon}} \equiv \boldsymbol{\sigma}_\varepsilon.\dot{\boldsymbol{\varepsilon}} \tag{5}$$

with $\boldsymbol{\sigma}$ represents the admissible stresses contained within the convex yield surface $\psi(\boldsymbol{\sigma})$ represents the stresses on the yield surface associated to any strain rates $\dot{\boldsymbol{\varepsilon}}$ through the plasticity condition.

The kinematic theorem of plasticity states that the structure will collapse if and only if there exists a kinematically admissible displacement field $\dot{\boldsymbol{u}} \in U$, such that

$$W_{int}(\dot{\boldsymbol{\varepsilon}}) < \lambda^+ W_{ext}(\dot{\boldsymbol{u}}) + W_{ext}^0(\dot{\boldsymbol{u}}) \tag{6}$$

where λ^+ is the collapse load multiplier, $W_{ext}^0(\dot{\boldsymbol{u}})$ is the work of any additional loads $\boldsymbol{f_o}$, $\boldsymbol{g_o}$ not subjected to the multiplier.

If defining $C = \{\dot{\boldsymbol{u}} \in U | W_{ext}(\dot{\boldsymbol{u}}) = 1\}$, the collapse load multiplier λ^+ can be determined by the following mathematical programming

$$\lambda^+ = \min_{\dot{\boldsymbol{u}} \in C} \int_\Omega D(\dot{\varepsilon}) d\Omega - W_{ext}^0(\dot{\boldsymbol{u}}) \tag{7}$$

IV. Brief on the Cell-Based Smoothed Finite Element Method (CS-FEM)

The essential idea of the cell-based smoothed finite element method (CS-FEM) combining the existing finite element method (FEM) with a strain smoothing scheme. In CS-FEM, the problem domain is discretized into elements as in FEM, such as $\Omega = \Omega^1 \cup \Omega^2 \cup ..... \cup \Omega^{nel}$ and $\Omega^i \cap \Omega^j = \varnothing, i \ne j$ the displacement fields are approximated for each element as

$$u^h(x) = \sum_{I=1}^{n} N_I(x) d_I \tag{8}$$

where n is the number of node per element and $d_I = [u_I \ v_I]^T$ is the nodal displacement vector.

Elements are then subdivided into several smoothing cells, such as shown in Fig. 2, and smoothing operations are performed for each smoothing cell (SC)

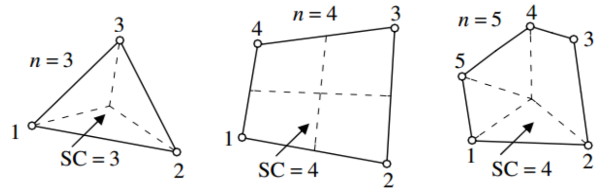

Figure 2. Smoothing cells for various element types: triangular element (left), quadrilateral element (middle) and polygonal element (right).

A strain smoothing formulation is given by [4]

$$\begin{aligned} \tilde{\varepsilon}^h(x_C) &= \int_{\Omega^e_C} \varepsilon^h(x) \varphi(x, x - x_c) d\Omega \\ &= \int_{\Omega^e_C} \nabla u^h(x) \varphi(x, x - x_c) d\Omega \end{aligned} \tag{9}$$

where $\tilde{\varepsilon}^h$ is the smoothed value of strains ε^h for smoothing cell $\Omega^e{}_C$ and φ is a distribution function or a smoothing function that has to satisfy the following properties [4]

$$\varphi > 0 \ and \int_{\Omega^e_C} \varphi d\Omega = 1 \tag{10}$$

For simplicity, the smoothing function φ is assumed to be a piecewise constant

$$\varphi(x, x - x_C) = \begin{cases} 1/A_C, & x \in \Omega^e{}_C \\ 0 \quad , & x \notin \Omega^e{}_C \end{cases} \tag{11}$$

where A_C is the area of the smoothing cell $\Omega^e{}_C$

Substituting (11) into (9), and applying the divergence theorem, one obtains the following equation

$$\tilde{\varepsilon}^h(x_C) = \frac{1}{A_C} \int_{\Omega^e_C} \nabla u^h(x) d\Omega = \oint_{\Gamma_C} n(x) u^h(x) d\Gamma \tag{12}$$

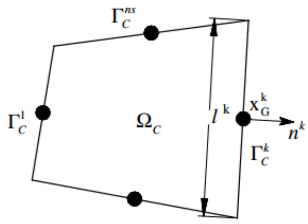

Figure 3. Geometry definition of a smoothing cell.

where Γ_c is the boundary of Ω^e_c and n is a matrix with components of the outward surface normal given by

$$n = \begin{bmatrix} n_x & 0 \\ 0 & \mathrm{n_y} \\ \mathrm{n_y} & n_x \end{bmatrix} \tag{13}$$

Introducing a finite element approximation of the displacement fields, the smooth version of the strain rates can be expressed as

$$\dot{\tilde{\varepsilon}}^{h}(\boldsymbol{x}_C) = \tilde{\boldsymbol{B}}\dot{\boldsymbol{d}} \tag{14}$$

where

$$\dot{\mathbf{d}}^T = [\dot{\mathrm{u}}_1, \dot{\mathrm{v}}_1, ...\dot{\mathrm{u}}_n, \dot{\mathrm{v}}_n] \tag{15}$$

$$\tilde{\mathbf{B}} = \begin{bmatrix} \tilde{N}_{1,x}(x_C) & 0 & ... & \tilde{N}_{n,x}(x_C) & 0 \\ 0 & \tilde{N}_{1,y}(x_C) & ... & 0 & \tilde{N}_{n,y}(x_C) \\ \tilde{N}_{1,y}(x_C) & \tilde{N}_{1,x}(x_C) & & \tilde{N}_{n,y}(x_C) & \tilde{N}_{n,x}(x_C) \end{bmatrix} \tag{16}$$

with

$$\begin{aligned} \tilde{N}_{I,\alpha}(x_C) &= \frac{1}{A_C}\int_{\Omega^e c} N_I(x) n_\alpha(x) d\Gamma \\ &= \frac{1}{A_C}\sum_{k=1}^{ns} N_I(x_G{}^k) n_\alpha{}^k l^k, I = 1, 2, ..., n \end{aligned} \tag{17}$$

where $\tilde{N}_{I,\alpha}$ is the smoothed version of shape function derivative $N_{I,\alpha}$; n_s is the number of edges of a smoothing cell Ω_c as shown in Fig. 3; x_G^k is the Gauss point of Γ_C^k boundary segment which has length l_x and outward surface normal n^k.

V. CS-FEM Formulation for Plane Strain with Mohr-Coulomb Yield Criterion

In this study, the Mohr-Coulomb failure criterion is used

$$\begin{aligned} \psi(\sigma) = \sqrt{(\sigma_{xx} - \sigma_{yy})^2 + 4\tau_{xy}{}^2} + ... \\ + (\sigma_{xx} + \sigma_{yy}) \sin\varphi - 2c\cos\varphi \end{aligned} \tag{18}$$

where c is cohesion and φ is internal friction angle of soil.

The plastic strains are assumed to obey the normality rule

$$\dot{\varepsilon} = \dot{\mu}\frac{\partial \psi}{\partial \sigma} \tag{19}$$

where the plastic multiplier $\dot{\mu}$ is non-negative.

Hence, the power of dissipation can be formulated as a function of strain rates for each domain i as [5]

$$D(\dot{\varepsilon}) = cA_i t_i \cos\varphi \tag{20}$$

where

$$\|\boldsymbol{\rho}\|_i \le t_i \tag{21}$$

$$\boldsymbol{\rho} = \begin{bmatrix} \rho_1 \\ \rho_2 \end{bmatrix} = \begin{bmatrix} \dot{\tilde{\varepsilon}}^h_{xx} - \dot{\tilde{\varepsilon}}^h_{yy} \\ \dot{\tilde{\gamma}}^h_{xy} \end{bmatrix} \tag{22}$$

$$\dot{\tilde{\varepsilon}}^h_{xx} + \dot{\tilde{\varepsilon}}^h_{yy} = t_i \sin\varphi \tag{23}$$

Introducing an approximation of the displacement and using the smoothed strains, the upper bound limit analysis for plane strain using the smoothed strains can be formed as

$$\lambda^+ = \min \sum_{i=1}^{n_{SD} x nel} cA_i t_i \cos\varphi \tag{24}$$

$$s.t \begin{cases} W_{ext}(\dot{u}^h) = 1 \\ \dot{u}^h = 0 \quad on\ \Gamma_u \\ \dot{\tilde{\varepsilon}}^h_{xx} + \dot{\tilde{\varepsilon}}^h_{yy} = t_i \sin\varphi \qquad i = 1, 2, \ldots, nel * n_{SD} \\ \|\rho\|_i \le t_i \qquad i = 1, 2, \ldots, nel * n_{SD} \end{cases} \tag{25}$$

where n_{SD} is the smoothing cell and nel is the number of element in the whole investigated domain. And the fourth constraint in problem (25), resulting optimization problem is cast in the form of a second-order cone programming (SOCP) problem so that a large-scale problem can be solved efficiently ([6-11]).

VI. Results and Discussion

In this study, the sizes of domain analysis need to ensure that the failures of slope only occur in chosen areas. Moreover, many cases considered to investigate the influence of many difference factors to the slope stability. An example for slope with the angle β = 30°, which shows boundary conditions and typical mesh, is illustrated in Fig. 4 with consists of 2270 four-node quadrilateral elements.

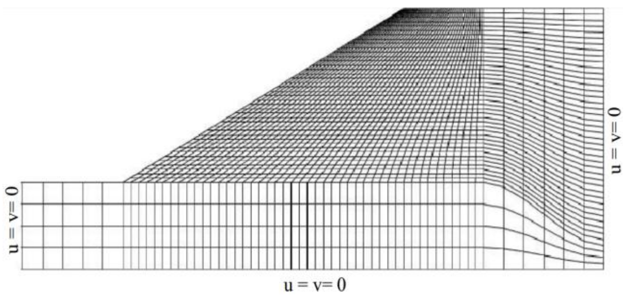

Figure 4. Typical mesh for the slope with β=30°.

A. *Horizontal Critical Seismic Coefficient (α_c)*

A slope with β = 30°, H = 20m and ϕ = 30° is described, assuming that vertical seismic loading is ignored. Various factors c/(γHtanϕ) from 0.022 to 0.303 were chosen to find out horizontal critical seismic coefficient (α_c). The result is compared with the result of [3]. The details are shown in Table I.

TABLE I. HORIZONTAL CRITICAL SEISMIC COEFFICIENT (A_C)

c/(γHtanϕ)	**Loukidis**		**CS-FEM**
	Lower bound	**Upper bound**	
0.022	0.111	0.145	0.124
0.043	0.181	0.220	0.192
0.087	0.291	0.331	0.305
0.173	0.464	0.504	0.478
0.260	0.593	0.631	0.612
0.303	0.646	0.678	0.669

It can be seen in Fig. 5 that the study's result is better than those of [3] with the same number of elements, about 2300. When compared to the average values of upper and lower bound limit analysis, the error provided by this analysis lies in the range of roughly 1% to 4%.

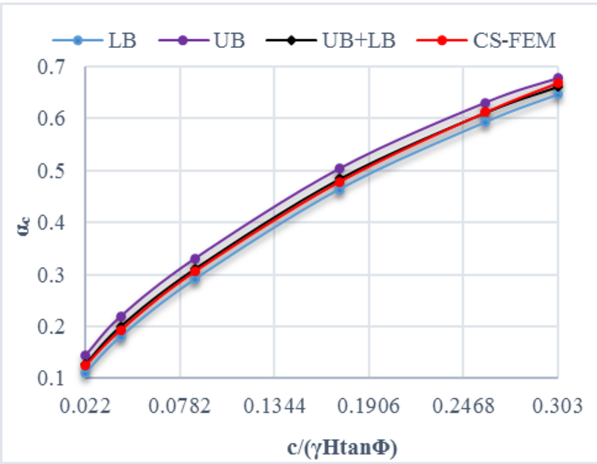

Figure 5. Comparison horizontal critical seismic coefficient

The patterns of plastic energy dissipation in the case c/(γHtanϕ) = 0.022 and 0.173 are shown in Fig. 6.

B. *Effect of the Slope Angle β*

A series of horizontal seismic coefficient α_h from 0.145 to 0.678 were chosen to considering the effect of the slope angle β on the stability. As expected, the stability factor γHtanϕ/c decrease as the slope angle or the horizontal seismic coefficient increase. The detail is shown in Table 2 as well as Fig. 7. It's easy to see that there are many differences in the stability when the horizontal seismic coefficient is small, namely, the stability factor of slope with β = 30° is much higher than those of β = 90° (about ten times). However, when the horizontal seismic coefficient is greater than 0.6, the stability factor seems not too much different.

Figure 6. Plastic dissipation distribution with c/(γHtanϕ) is 0.022 and 0.173.

TABLE II. THE STABILITY FACTOR OF SLOPE ΓHTANϕ/C

α_c	β			
	30	45	60	90
0.145	35.475	10.789	6.420	3.145
0.220	18.973	8.331	5.410	2.815
0.331	10.287	6.013	4.289	2.400
0.504	5.413	3.948	3.105	1.896
0.631	3.755	3.024	2.504	1.627
0.678	3.344	2.759	2.322	1.544

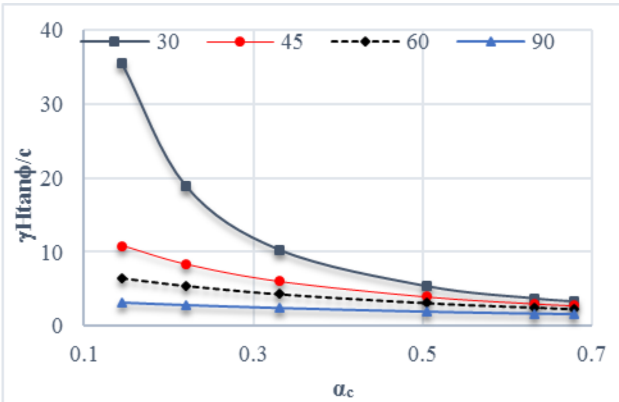

Figure 7. The slope stability for different cases of β

a)

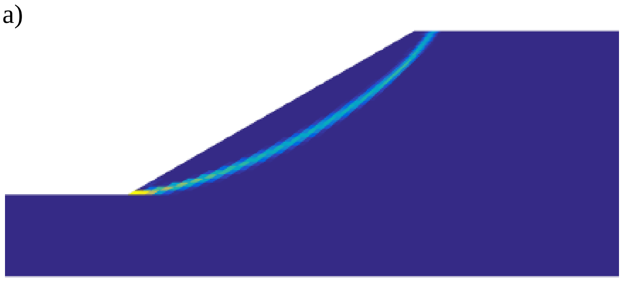

b)
c)
d)

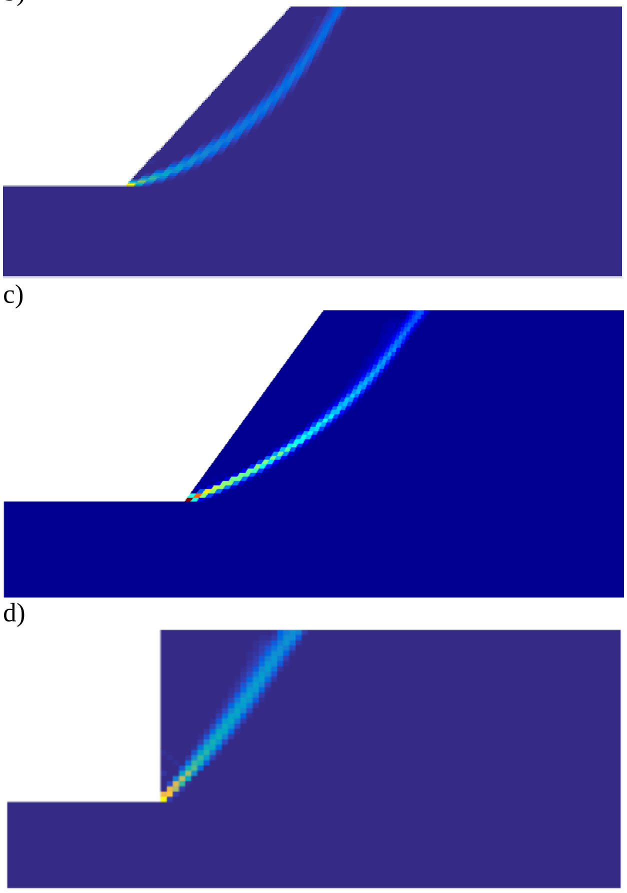

Figure 8. Plastic dissipation distribution for the case α_c=0.145 and a) β=30^o ,b) β=45^o,c) β=60^o and d) β=90^o.

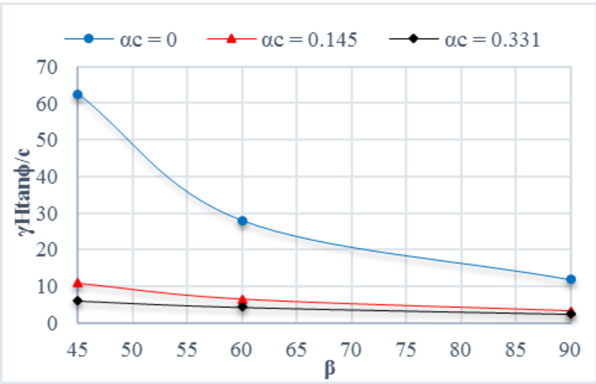

Figure 9. Comparison the stability of slope in static and seismic conditions.

The patterns of plastic energy dissipation for the case β=30^o, 45^o, 60^o and 90^o and α_c=0.145 are shown in Fig. 8.

In order to more general about the effect of earthquake to the stability of slope, Fig. 9 compares the stability factor ($\gamma H\tan\phi/c$) in static ~~conditions~~ with two cases α_c=0.145 and α_c=0.331 in three different values β, namely, 45^o, 60^o and 90^o. When compared to the case α_c=0.145, the stability of slope in static conditions is greater than 3.7-5.8 times. Although, the horizontal seismic coefficient increases more than doubled, from 0.145 to 0.331, the stability factor only decreases less than twice, about 1.31-1.79 times.

VII. Conclusion

A novel procedure for performing upper bound limit analysis using cell-based smoothed finite element method (CS-FEM) and second-order cone programming (SOCP) has been described. The key advantage of applying the CS-FEM to limit analysis problems is that the size of optimization problem is reduced. Various numerical examples were presented to show that the presented method can provide accurate and stable solution.

The effect of pseudo-static seismic forces on the stability of slope has been adopted. The seismic stability factors are presented in the tables as well as compared with other solutions in the graphics. The results obtained should be useful for designing foundations in a seismically active zone.

Acknowledgment

The authors would like to express our sincere thanks to Assoc. Prof. Dr. Canh V. Le who developed code for the cell-based smooth finite element combine with the second-order cone programming and deep gratitude to MSc. Hoang C. Nguyen who developed this theory for the soil model. This is fundamental to this study.

References

[1] O. Kusakabe, T. Kimura, and H. Yamaguchi, "Bearing capacity of slopes under strip loads on the surfaces," in *Proc. 1981 Soils and Foundations Conf.*, 1981, pp. 29-40.

[2] J. S. Shiau, R. S. Merifield, A. V. Lyamin, and S. W. Sloan, "Undrained Stability of Footings on Slopes," in *Proc. 2011 International Journal of Geomechanics Conf.*, 2011, pp. 381-390.

[3] D. Loukidis, P. Bandini, and R. Salgado, "Stability of seismically loaded slopes using limit analysis," in *Proc. 2003 GÉOtechnique Conf.*, 2003, pp. 463-479.

[4] G. R. Liu, T. T. Nguyen, K. Y. Dai, and K. Y. Lam, "Theoretical aspects of the smoothed finite element method (SFEM)," in *Proc. 2007 International Journal for Numerical Methods in Engineering Conf.*, 2007, pp. 902-930.

[5] A. Makrodimopoulos and C. M. Martin, "Upper bound limit analysis using simplex strain elements and second-order cone programming," in *Proc. 2007 International Journal for Numerical and Analytical Methods in Geomechanics Conf.*, 2007, pp. 835-865.

[6] C. V. Le, et al, "A cell-based smoothed finite element method for kinematic limit analysis," in *Proc. 2010 International Journal for Numerical Methods in Engineering Conf.*, 2010, pp. 1651-1674.

[7] C. V. Le, M. Gilbert, and H. Askes, "Limit analysis of plates using the EFG method and second-order cone programming," in *Proc. 2009 International Journal for Numerical Methods in Engineering Conf.*, 2009, pp. 1532-1552.

[8] G. R. Liu, T. T. Nguyen, and K. Y. Lam, "An edge-based smoothed finite element method (ES-FEM) for static, free and forced vibration analyses of solids," in *Proc. 2008 Journal of Sound and Vibration Conf.*, 2008, pp. 1100-1130.

[9] H. X. Nguyen, G. R. Liu, T. T. Nguyen, and C. T. Nguyen, "An edge-based smoothed finite element method for analysis of two-dimentional piezoelectric structures," in *Proc. 2009 Smart Materials and Structures Conf.*, 2009.

[10] H. C. Nguyen, "Limit analysis on soil using edge-base smooth finite element method and mathematical optimization," M.S. thesis, Dept. Civil. Eng., Vietnam National Univ., HoChiMinh, Vietnam, 2012.

[11] Mosek, The MOSEK optimization toolbox for MATLAB manual, http://www.mosek.com.

Hai N. Le Dong Nai, VietNam, 10/01/1991. Bachelor of Civil Engineering, Civil Engineering, Ho Chi Minh City University of Technology, Ho Chi Minh, Vietnam, 2014.

From 3/2014 to 1/2015, he was a STRUCTURAL ENGINEER at Hoa Binh Construction & Real Estate Corporation, Ho Chi Minh, Vietnam. From 1/2015 to now, he has been a MASTER STUDENT at Ho Chi Minh University of Technology, Ho Chi Minh, Vietnam. Computational Mechanics, Computational Plasticity (Limit Analysis), Numerical Methods (Finite Element Method, SFEM, Isogeometric Analysis…).

An N. Chau Long An, Vietnam, 26/11/1952. Bachelor of Civil Engineering, Civil Engineering, Ho Chi Minh City University of Technology, Ho Chi Minh, Vietnam, 1974. Master of Engineering, Soil Mechanics and Material Mechanics, Institut National Polytechnique de Grenoble, Grenoble, France, 1995. Doctor of Philosophy, Soil Mechanics and Material Mechanics, Institut National Polytechnique de Grenoble, Grenoble, France, 1999. Associate Professor, Vietnam, 2006.

From 1999 to the present, he has been a SENIOR LECTURER at Ho Chi Minh City University of Technology, Ho Chi Minh, Vietnam. He published two books: Soil Mechanics (Ho Chi Minh, Ho Chi Minh City Vietnam National University Publishers, 2011), Foundation (Ho Chi Minh, Ho Chi Minh City Vietnam National University Publishers, 2011). Research interests of him: behavior of soil and bulk material, behavior of weak soil and soil cement mixer…